ARMA/NARMS 04-487

Controls on Oil And Gas Distribution in Over-Pressured Reservoirs

Susan Hippler
ExxonMobil Exploration Company, Houston, Texas

Thomas Finkbeiner
GeoMechanics International, Mainz, Germany

Amie Lucier
Department of Geophysics, Stanford University, Stanford, California

Mark D. Zoback
Department of Geophysics, Stanford University, Stanford, California

ABSTRACT: Distribution of overpressure and hydrocarbon phases in the Eugene Island Block 330 Field, Gulf of Mexico, support previous suggestions that episodic slip on critically stressed faults provides dynamic control of hydrocarbon column heights in some of the fault blocks. On the hanging-wall of the field's growth fault system, pore pressures in the OI reservoir at the top of the structure are noticeably higher than porosity-based pressure predictions for the top seal. In addition, water phase pressures in the reservoir vary markedly from fault block to fault block, implying significant differences in reservoir plumbing. Fault blocks with relatively lower water phase pressures contain large gas columns with small oil rims. Down-flank spill or leak points control the total column height, while capillary seal capacity limits the amount of gas. In this situation, gas leaks at the crest of the structure and is unable to flush oil out of the trap. In contrast, fault blocks with markedly higher water phase pressures are significantly under-filled, and contain small oil columns. As the pressure at the top of the columns are within ≥92% of the least principal stress, we propose that critically stressed faults control trap fill. In this scenario, any additional hydrocarbon charge increases pressure, inducing slip on bounding faults and causing gas leakage from the trap leaving an oil column behind.

1. INTRODUCTION

Post-drill analysis of hydrocarbon fields world-wide indicates that controls on trap fill can be classified broadly into two main categories: geologic controls and dynamic controls. Under hydrostatic conditions, capillary entry pressure is the dominant geologic control on hydrocarbon migration and entrapment in the subsurface [1]. Sales [2] showed that capillary entry pressure can control not only the total hydrocarbon column height a trap holds, but also oil and gas column heights. Similarly, this paper shows that dynamic mechanisms that control total trap fill (hydraulic fracturing and dynamic fault capacity) can also control oil and gas distribution in hydrocarbon bearing reservoirs.

2. DYNAMICALLY CONSTRAINED HYDROCARBONS

Areas undergoing rapid sedimentation like the Gulf of Mexico are often characterized by a normal faulting environment where the overburden is the maximum principal stress (i.e., $S_{hmin} \leq S_{Hmax} \leq S_v$). In such areas the pore pressures in compacting shales are generally expected to be higher than in adjacent sands units because of their low permeability and relatively poor drainage during compaction. However, there have also been models published predicting the contrary (i.e., pore pressures in sands are higher than in adjacent shales) under appropriate circumstances. The centroid as presented by Traugott and Heppard [3] is such a model. Finkbeiner et al. [4] proposed a modified version of this model that uses pore pressures values at the top of reservoir sands and integrates this pressure information with the ambient in situ state of stress in the shales to evaluate dynamic mechanisms for fluid migration

and accumulation. These mechanisms enable us to establish bounds for the maximum column heights supported by the fluids trapped in the reservoir since it is the sealing capacity of the overlaying top seal or the fault against which the reservoir abuts that controls a critical pore pressure in the underlying sand.

In this paper we are focusing on dynamic capacity. In other words, frictional failure along optimally oriented, pre-existing faults. This failure occurs when the shear stress resolved along the fault plane overcomes its frictional resistance and the fault slips. The critical pore pressure in the sand underlying the sealing fault that drives this mechanism is not required to be as high as the least principal total stress in the overlying shale. Hence, the least principal effective stress in the shale has a finite, positive value and is a function of the frictional properties (μ) of the slipping fault. Notice that a necessary condition for this dynamic mechanism to operate is for the pore pressure in the sand to be higher relative to the overlying shale, since it is the pressure in the underlying sand that has to induce failure in the overlying shale (i.e., breach of seal) for fluid flow to occur.

In Figure 1 we illustrate the dynamic capacity model in the light of a sand reservoir that is filling over time with oil or gas until the hydrocarbon column has reached a specific height. The maximum column the reservoir sand can support depends on (i) the initial water phase pressure in the reservoir, (ii) the mechanisms by which fluids migrate, and (iii) the density of the hydrocarbon phase. When the reservoir sand has low initial water phase pore pressures large hydrocarbon columns can accumulate over time before the dynamic capacity (i.e., P_p^{crit}) is reached. In contrast, when the reservoir sands have high initial water phase pore pressures the dynamic reservoir capacity is reached at much earlier times and relatively smaller hydrocarbon columns develop. If the reservoir has not reached its dynamic capacity because the observed hydrocarbon column is small and not in dynamic equilibrium, we can conclude that the reservoir is either still filling, has a spill point, or is leaking (i.e., statically controlled fluid flow).

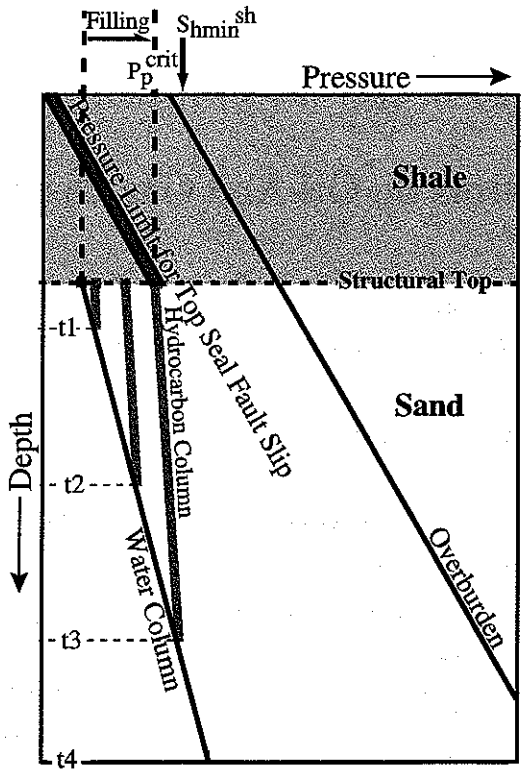

Fig. 1. Conceptual model of filling a sand reservoir with hydrocarbons (gray columns) as a function of initial water pressure (black) and time (outlined with three time steps t_1 through t_3). The critical pore pressure (i.e., P_p^{crit}; wide gray line) is the maximum capacity of the reservoir beyond which fluid flow occurs along the reservoir bounding fault during slip events.

Under the assumption of the dynamic capacity model, hydrocarbon column heights are potentially controlled by the state of stress at the reservoir-fault contact in a manner that when the pore pressure at the top of the sand reaches the value required for the fault to fail in the shale (P_p^{crit}) an episode of fluid flow occurs. In this scenario, the reservoir has reached its maximum hydrocarbon column and is at dynamic capacity. In other words, the hydrocarbon column in the reservoir is in dynamic equilibrium with the state of stress in the overlying shale top seal. Note also that as the maximum pore pressure is reached at the crest of the trap, the most buoyant hydrocarbon phase will be leaking preferentially in this situation.

3. EUGENE ISLAND BLOCK 330

The Eugene Island Field is located about 160 km offshore Louisiana in the Gulf of Mexico [5]. Recoverable reserves have been estimated at 307 million bbl of liquid hydrocarbons and 1.65 tcf of gas, which are distributed in more than 25 different reservoirs, segmented by shales and normal faults.

We focus our analysis on the reservoirs of the OI-1 sand. The OI-1 is bounded by a concave shaped, predominantly NW-SE striking sequence of normal faults that constitute the main basin bounding growth fault system in the field.

On the downthrown side within the mini-basin, several approximately E-W striking normal faults subdivide the system into at least 5 different fault blocks that are sequentially labeled "A" through "E". The offset along these normal faults is approximately of 30.5 m (=100 ft.) (antithetic and subsidiary faults) to 243.9 m (= 800 ft.) (main basin bounding growth fault).

Fault blocks A, D, and E exhibit small oil columns (dark gray) of between 152.4 m (= 500 ft.) and 167.7 m (= 550 ft.). In contrast, the total column heights in B and C are quite large 640.2m ((= 2,100 ft.) and 457.3 m (=1,500 ft.) respectively) and characterized by long gas and relatively short oil columns.

3.1. Fluid pressure distribution

Pore pressure data within the reservoir sands were obtained from repeat formation tests (RFT) and bottom hole pressures (BHP). We used the earliest pressure records in the reservoir sands to get the pore pressure conditions prior to production while the reservoir was in an undepleted state. Given pore pressures at some level within the reservoir sand, we calculated live fluid densities following the method by Batzle and Wang [6] and extrapolated the reservoir pressures to the structural tops.

The OI-1 is moderately to severely overpressured and there exist significant differences in the hydrocarbon phase pressures and the water phase pressures in the various OI-1 fault blocks. The hydrocarbon phase pressure at the top of the structures in fault blocks B and C are apparently equal whereas the oil phase pressures at the top of fault blocks A and E are significantly higher. This is true even though the column heights are much larger in fault blocks B and C and the structural tops are at different depths. Furthermore, if we look at the water pressure at an equivalent depth, we see that there are sharp differences. Pressures in fault blocks B and C are 3.45 MPa to 4.83 MPa (500 to 700 psi) lower than in fault blocks A and E.

Predicted shale pore pressures (P_p^{sh}) were calculated from a porosity-effective stress method based on sonic log data [7, 8]. We extrapolated the pressure values through linear regressions to the top of the reservoir sands. In all cases, at the peak of the structure, the shale pressure is considerably less than the sand pressure (i.e., between 15% and 25%), which fulfills a necessary requirement for the dynamic capacity mechanisms to operate. Furthermore, shale pressures mirror the water phase pressures recorded in the sand. At a given depth shale pressures are lower in fault blocks B and C than in fault blocks A and E. Figure 2 illustrates these facts.

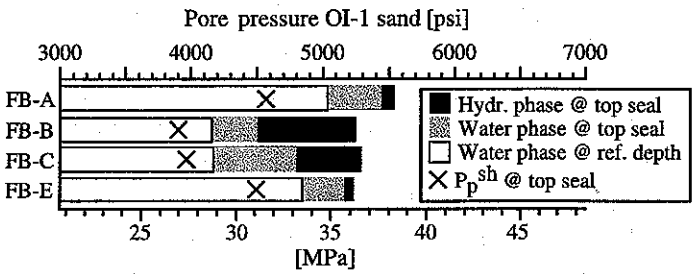

Fig. 2. In-situ pore pressure conditions at the top of the OI-1 fault blocks. Hydrocarbon (black column) and water (gray column) phase pore pressure at top of the reservoirs (seal top). The difference between both indicates hydrocarbon column height. The white column displays the water phase pore pressure at a specific reference datum (i.e., 1829m or 6,000 ft. SSTVD). The cross shows the shale pressure (P_p^{sh}) at the top of each reservoir block.

3.2. Stress conditions

The overburden stress (S_V) was calculated utilizing an average gradient derived from integrating density logs. The overburden gradients for all wells range between 20.5 MPa/km (= 0.91 psi/ft) and 21.2 MPa/km (= 0.94 psi/ft). The calculations are associated with an uncertainty of approximately 0.3 MPa/km (= 0.015 psi/ft) or 1.7% based on determination of the overburden in several wells.

The minimum principal stress in the top seal (S_{hmin}^{sh}) was determined based on leak-off test (LOT) and formation integrity test (FIT) measurements. In contrast to LOTs, FITs do not hydraulically fracture the formation, hence, they generally present a lower bound for the minimum principal stress. Similar to the shale pore pressure data, we used linear regressions to extrapolate S_{hmin}^{sh} to the structural highs

The least principal stress in the shale (S_{hmin}^{sh}) lies approximately 80% of the distance between the shale pressure (P_p^{sh}) and the overburden (S_v). This trend is well established in fault blocks A and B where multiple stress measurements were made in the vicinity of the OI-1 horizon. We inferred the S_{hmin}^{sh} trend in fault blocks C and E from adjacent

fault block B because there is none or only one LOT available.

4. DISCUSSION

For the various fault blocks of the OI reservoir we carefully examine pore pressures at their structural tops, in-situ stress of the overlying shale caps, and hydrocarbon column heights. Utilizing these data, we determine the critical pore pressure value (P_p^{crit}) based on Coulomb frictional failure theory [9]. We calculate an upper and lower bound for P_p^{crit} using two different values for the coefficient of friction (μ) that seem reasonable for the SEI 330 field: (i) $\mu = 0.3$ (lower bound) and (ii) $\mu = 0.6$ (upper bound). The lower bound results from laboratory experiments with clay under undrained conditions [10, 11]. The upper bound, in contrast, is a typical value found in field measurements in many areas around the world [12 – 14]. Second, we compare the pore pressure at the top of each reservoir sand to the range of P_p^{crit} values and draw some implications about fluid flow and the observed hydrocarbon column heights in each of the reservoirs.

Hence, the critical pore pressures (P_p^{crit}) of a reservoir represents a state of dynamic equilibrium for which failure and fluid migration would occur (through slip of the reservoir bounding fault. In other words, this critical value defines the maximum column height (i.e., pore pressure) at which a reservoir has reached its dynamic capacity.

In Figure 3, we display the current pressure and stress conditions at the top of the four OI-1 sand fault blocks. These figures provide the basis for the following discussion.

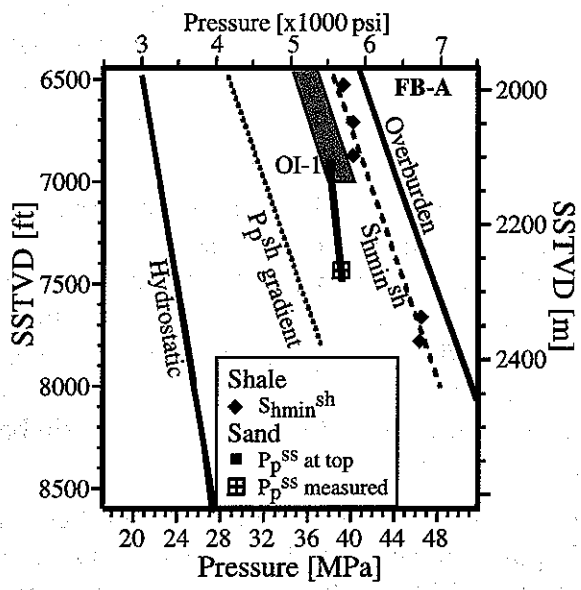

(a)

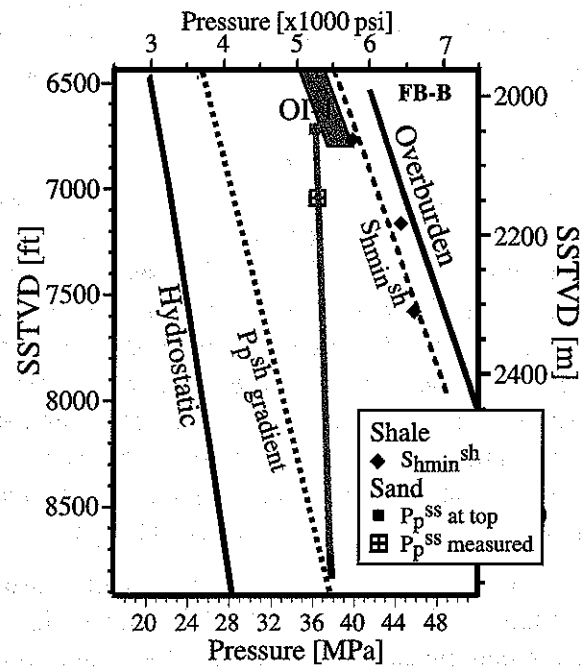

(b)

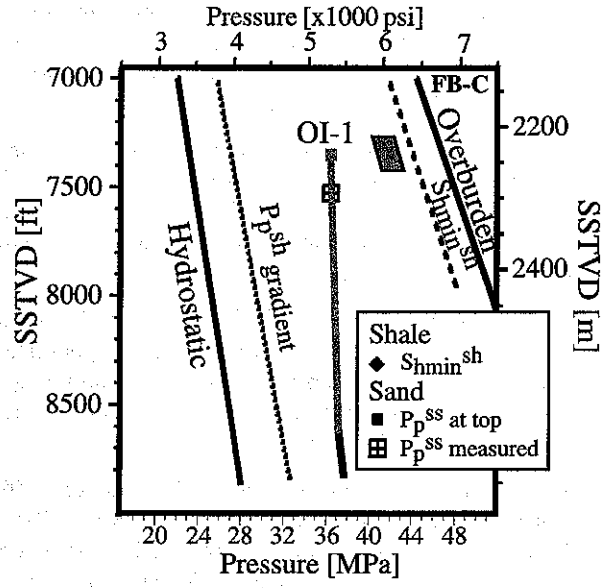

(c)

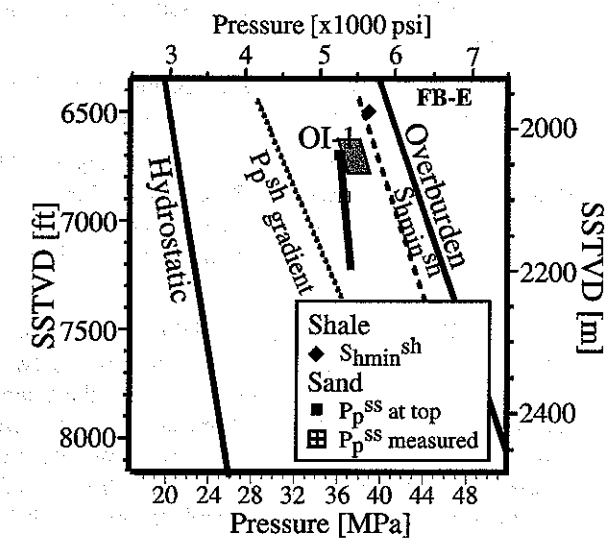

(d)

Fig. 3. Pressure and stress state in the four fault blocks (FB; a) FB-A, b) FB-B, c) FB-C, d) FB-E) of the OI-1 sand. Least principal stresses in shales (S_{hmin}^{sh}) are from leak-off tests (LOT) and formation integrity tests (FIT). We also display the regression line for shale pore pressures (short dashes) and reservoir pore pressures (P_p^{ss}). The black squares represent P_p^{ss} at the top of each sand (black for oil phase, gray for gas phase) calculated by using live oil gradients. Solid lines represent hydrostatic and lithostatic gradients and the dashed lines are linearly regressed gradients for P_p^{sh} and S_{hmin}^{sh}. The gray area paralleling the trends for least principal stress in the shale and the overburden indicates the range of critical pore pressures (for friction values between 0.3 and 0.6) for which the top seal reaches its frictional limit, the reservoir bounding fault slips, and the reservoir is at dynamic capacity.

In all fault blocks, hydrocarbon phase pore pressures at the peak of the OI-1 structure are lower than the least principal stress in the shale (i.e., the difference between S_{hmin}^{sh} and P_p^{ss} is not zero). Consequently, the reservoirs are not at hydraulic fracturing conditions. However, fault blocks A and E exhibit relatively high pressures and short oil columns at their tops. Pore pressures are either well within or just at the limit of dynamic equilibrium, which indicates that the two reservoirs are at their dynamic capacity (i.e., the oil columns have reached their maximum height) as controlled by the ambient state of stress. Thus, dynamic mechanisms for hydrocarbon migration and accumulation are operating today in this part of the reservoir and the minibasin bounding growth fault at this stratigraphic level can be characterized as potentially active (this conclusion is further confirmed through observed stress induced borehole breakouts; unpublished data). In these two fault blocks, initial aquifer pore pressure conditions were quite high in the past, allowing gas to leak preferentially from the trap crests and only relatively small amounts of oil to accumulate, thus, limiting total trap fill. In fault blocks B and C, the columns are much longer and pore pressures are (just) below dynamic equilibrium. Pore pressure data suggest that fault block B is in hydraulic communication with C. It appears that the columns in fault blocks B and C are static and controlled by the presence of a spill point (i.e. leakage below dynamic capacity). In fact, this spill point exists down dip and to the west in fault block C and is approximately equivalent to the mapped oil-water contact implying that hydrocarbons can migrate westward into the 331 structure [15]. The long gas columns in these two fault blocks (B and C) reflect relatively low initial pore pressures in the past, allowing for large gas columns with small oil rims to develop.

In the OI-1, we also identify an interesting correspondence between aquifer pore pressures and column heights. Low shale and sand aquifer pressures are associated with large, dominantly gas columns (fault blocks B and C), whereas fault blocks A and E exhibit relatively high aquifer pressures and short oil columns. Figure 1 provides an explanation for this scenario. In environments of high initial aquifer pressures, the difference between P_p^{crit} and the sand pressure is small, the reservoir can support more of less buoyant hydrocarbon phases, and P_p^{crit} can be reached much quicker. Conversely, if initial aquifer pressures are relatively low, the difference between P_p^{crit} and P_p^{ss} is large, the reservoir supports a long hydrocarbon column, and P_p^{crit} could be reached at a later time.

The fact that such drastic differences in sand and shale pore pressures can exist in adjacent fault blocks of the same sand (i.e., the OI-1) is very interesting but also quite puzzling. Since water phase pore pressures in fault blocks B and C are similar, they are hydraulically connected to the same aquifer but decoupled from fault blocks A and E as inferred from the large pressure contrast. Because the shale pressures adjacent to the OI-1 reservoirs show similar contrasts, the same mechanisms operating in the sands probably also affected the shales. We believe, therefore, that during burial and structural evolution of the OI-1 sand a very effective compartmentalization process allowed hydraulic decoupling of the aquifer in these fault blocks and substantial different aquifer pore pressure regimes to develop. Pressure compartmentalization in sedimentary basins as observed in the OI-1 sand is described with numerous case studies by Powley [16] and Hunt [17].

5. CONCLUSIONS

We introduced the dynamic capacity model to explain a characteristic distribution of hydrocarbon columns in different fault blocks of the moderately overpressured OI-1 sand in the South Eugene Island Field, Gulf of Mexico. This sand reveals two interesting points: (i) the oil columns in fault blocks A and E are short and exhibit high pressures at the top of the columns that are within ≥92% of the least principal stress. We propose that these pressures are close to the values expected for dynamic fault slip and that critically stressed faults control trap fill. In this scenario, any additional hydrocarbon charge increases pressure, inducing slip on bounding faults and causing gas leakage from the trap leaving an oil column behind. Thus, these two reservoir compartments are at dynamic capacity today and column heights and fluid migration are controlled by active faulting. (ii) While the OI-1 reservoirs in fault blocks B and C exhibit very long hydrocarbon columns, pressures are below dynamic equilibrium. There is good evidence that the hydrocarbon phases in these fault blocks are spill point controlled and hydrocarbons can escape into the westward structure of the OI-1.

REFERENCES

1. Schowalter, T.T., 1979, Mechanics of secondary hydrocarbon migration and entrapment: AAPG Bulletin. 63: 723-760.
2. Sales, J.K., 1997, Seal strength vs. trap closure – a fundamental control on the distribution of oil and gas, in R. C. Surdam, ed., Seals, traps and the petroleum system. AAPG Memoir 67: 57-83.
3. Traugott, M.O., and P. D. Heppard, 1994, Prediction of pore pressure before and after drilling - taking the risk out of drilling overpressured prospects: American Association of Petroleum Geologists Hedberg Research Conference, Golden Colorado, June 8-10.
4. Finkbeiner, T., M. Zoback, P. Flemings and B. Stump. 2001. Stress, pore pressure and dynamically constrained hydrocarbon columns in the South Eugene Island 330 field, northern Gulf of Mexico. *AAPG Bulletin.* 85: 1,007-1,031.
5. Holland, D.S., J. B. Leedy, and D. R. Lammlein, 1990, Eugene Island Block 330 field - USA, offshore Louisiana, *in* E. A. Beaumont, and N. H. Foster, eds., Structural traps III, tectonic fold and fault traps: American Association of Petroleum Geologists, Treatise of Petroleum Geology Atlas of Oil and Gas Fields, p. 103-143.
6. Batzle, M., and Z. Wang, 1992, Seismic properties of pore fluids: Geophysics, v. 57, p. 1396-1408.
7. Hart, B.S., P. B. Flemings, and A. Deshpande, 1995, Porosity and Pressure: Role of Compaction Disequilibrium in the Development of Geopressures in a Gulf Coast Pleistocene Basin: Geology, v. 23, p. 45-48.
8. Stump, B. B., P. B. Flemings, T. Finkbeiner, and M. D. Zoback, 1998, Pressure differences between overpressured sands and bounding shales of the Eugene Island 330 field (offshore Louisiana, USA) with implications for fluid flow induced by sediment loading, *in* Mitchell, A., and D. Grauls, eds., Overpressures in petroleum exploration: workshop proceedings, April 7-8, Pau, France, p. 83-92.
9. Jaeger, J. C., and N. G. W. Cook, 1979, Fundamentals of rock mechanics (3d ed.): New York, Chapman and Hall, p. 28-30.
10. Wang, C.Y., N. Mao, and F. T. Wu, 1979, The mechanical property of montmorillonite clay at high pressure and implication on fault behavior: Geophysical Research Letters, v. 6, p. 476-478.
11. Wang, C.Y., N. Mao, and F. T. Wu, 1980, Mechanical properties of clays at high pressures: Journal of Geophysical Research, v. 85, p. 1,462-1,468.
12. Zoback, M.D, and J. H. Healy, 1984, Friction, faulting, and in-situ stress: Annales Geophysicae, v.2, p. 689-698.
13. Zoback, M.D, and J. H. Healy, 1992, In situ stress measurements to 3.5 km depth in the Cajon Pass scientific borehole: implications for the mechanics of crustal faulting: Journal of Geophysical Research, v. 97, p. 5,039-5,057.
14. Brudy, M., M. D. Zoback, K. Fuchs, F. Rummel, J. Baumgaertner, 1997, Estimation of the complete stress

tensor to 8 km depth in the KTB scientific drill holes: Implications for crustal strength: Journal of Geophysical Research, v. 102, p. 18,452-18,475.

15. Rowan, M.G., B. S. Hart, S. Nelson, P.B. Flemings, and B. D. Trudgill, 1998, Three-dimensional geometry and evolution of a salt-related growth-fault array: Eugene Island 330 field, offshore Louisiana, Gulf of Mexico: Marine Petroleum Geology, v. 15, p. 309-328.

16. Powley, D.E., 1990, Pressures and hydrogeology in petroleum basins: Earth-Science Reviews, v. 29, p. 215-226.

17. Hunt, J.M., 1990, Generation and migration of petroleum from abnormally pressured fluid compartments: American Association of Petroleum Geologist Bulletin, v. 74, p. 1-12.